

STRONG SUPPRESSIONS OF SURFACE WATER AT LUNAR MAGNETIC ANOMALIES SEEN BY THE MOON MINERALOGY MAPPER (M³) DATA. S. Li¹ and I. Garrick-Bethell^{2,3}, ¹Hawai'i Institute of Geophysics and Planetology, University of Hawaii; ²Department of Earth and Planetary Sciences, University of California; ³School of Space Research, Kyung Hee University, Seoul, South Korea. shuaili@hawaii.edu

Introduction: Evidence from lunar returned Apollo samples [1], spacecraft measurements [2-5], and ground-based telescopic observations [6] all supports the presence of water (OH/H₂O, herein referred to as water) on the lunar surface. However, the origins of the lunar surface water are still enigmatic. Determining the origins of water in lunar returned Apollo samples was complicated by terrestrial contamination [7]. The hydrogen isotope (D/H) of water quenched in Apollo agglutinate samples with no terrestrial contamination shows that most of observed water could have originated from solar wind implantation [1]. However, it is unclear whether the sources of water seen in Apollo samples represent the global lunar surface. Furthermore, recent studies suggest that the amount of water degassed from the lunar interior may be sufficient to account for the water observed on the lunar surface [8]. The possibility of water liberated from the surface by exospheric dust impacts [9] also complicates assessing the origins of the lunar surface water.

Lunar lithospheric magnetic anomalies provide a natural laboratory for examining the role of the solar wind flux in water production. The magnetism at most of these locations likely formed several billions of years ago [10]. Regardless of their origin, the Moon's strongest magnetic anomalies likely reduce the surface solar wind flux [10], while vertical field structures may channel more solar wind flux and energy to the surface [11]. Hence, magnetic anomalies systematically reduce/enhance solar wind flux and energy depending on the structure of the magnetic field, while locally keeping other confounding variables constant (e.g. temperature, UV photon flux, and impacts).

Changes in solar wind protons reaching the surface may produce variations in lunar surface water content [12], if the contribution of water from impacts and

interior degassing is constant in that region and represents a background water signal. Thus, assessing whether water content is suppressed at magnetic anomalies may reveal how much contribution is from solar wind implantation. Here the correlation of water content and magnetic fields is examined.

Data & Methods: We map the lunar surface water content using the Moon Mineralogy Mapper (M³) data. The same mapping algorithm is used as that in [13]. We estimate that the uncertainty of our mapped water content is ~20 ppm [13] based on the signal to noise ratio provided in [14]. In this work, we add 20 ppm to our estimated water content for each M³ pixel to avoid non-physical negative values of water abundance. We then mosaic the global water map from all five optical periods (OPs) M³ data at a spatial resolution of ~280 m/pixel

We use the magnetic field data that were derived from Kaguya and Lunar Prospector observations by [15]. We expanded their spherical harmonic model at degree and order 450 at an altitude of 20 km. The magnetic field uncertainty is less than ~1 nT [15]. A map of the total field strength was generated at a resolution of 8 ppd. This resolution is an oversampling of the intrinsic resolution of the model by about a factor of 5. The resulting map is a smoothed, interpolation of the field data, which facilitates comparisons to the much higher resolution M³ data.

Results: Strong water suppressions are seen at the three magnetic anomalies examined (**Fig. 1**). The azimuthally averaged water content and total magnetic field strength are plotted as a function of distance from the centers of each magnetic anomaly at Reiner Gamma, Airy, and Gerasimovich anomalies (**Fig. 2**). The centers of magnetic anomalies at Reiner Gamma, Airy, and

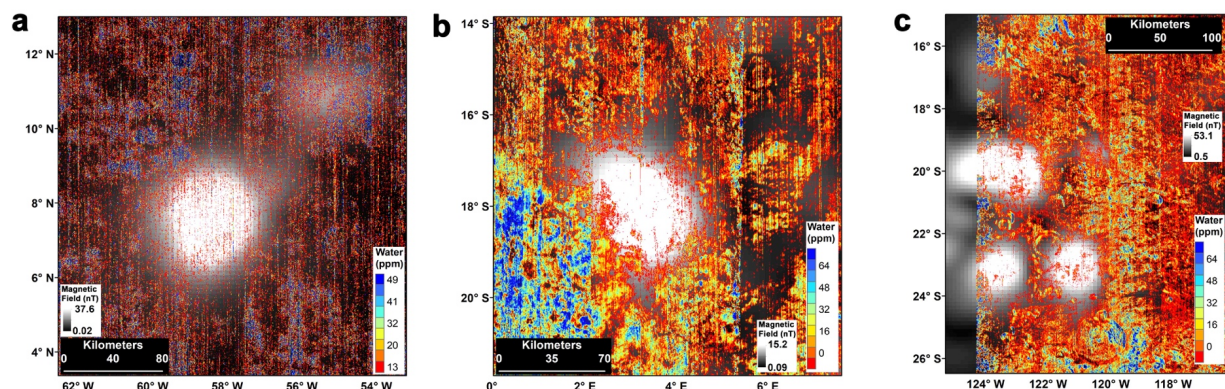


Fig. 1. Water maps overlain on magnetic fields at Reiner Gamma (a), Airy (b), and Gerasimovich (c). This figure is modified from Fig. 2-4 in [19].

Gerasimovich exhibit ~ 0 ppm water (**Fig. 2a-c**), and the water content increases sharply approaching regions outside the anomalies. The average water contents outside of Reiner Gamma, Airy, and Gerasimovich are ~ 15 ppm, ~ 25 ppm, and ~ 20 ppm, respectively (**Fig. 2**). The strongest magnetic fields at Reiner Gamma, Airy, and Gerasimovich are 37 nT, 15 nT, and 46 nT, respectively (**Fig. 2**), while the magnetic field strength outside of magnetic anomalies are close to 0 (**Fig. 2**).

Discussion: Previous studies suggest that the absorption strength of water bands near $3 \mu\text{m}$ is dependent on temperatures used for correcting the thermal effects of M^3 data [13, 16-18]. False water absorptions may be present if the thermal effect of M^3 data is overestimated [19]. However, this should not be a concern in this study. Our calculations suggest that unreasonably higher temperatures would be required at the three magnetic

anomalies to create similar water absorptions in M^3 data as the surrounding terrains [19]. Furthermore, the suppression of water is seen not just across the high albedo swirls, but over the broader, circular shaped magnetic field map outside the swirl, in contrast to previous reports where water content is correlated with the swirl pattern [12, 13]. There is no reason to believe that regions of strong magnetic field should be much warmer than their surroundings at similar latitudes, surface roughness, albedo, and time of day. These results suggest that the strong suppression of water content at these magnetic anomalies is real and cannot be introduced by the thermal correction or other nuances of the M^3 data set.

The bright optical patterns at swirls are not strongly correlated with the water suppressions, suggesting the energies and fluxes required to produce each of these phenomena are different, and not completely understood.

Conclusion: The overall correlation between water content and magnetic field suggests that a significant component of the lunar surface water may originate from solar wind implantation. The lack of detectable water features in the three anomalies studied here suggest that most impact delivered water cannot be retained. Further missions (e.g. [20]) and studies are required to understand how the magnetic shielding effect occurs at the surface. This is critical for quantitatively understanding the formation of solar wind induced water on the Moon and other airless bodies such as Mercury, Vesta, and asteroids.

References: [1]. Liu *et al.*, (2012), *Nat. Geo.*, 5. [2]. Sunshine *et al.*, (2009), *Science*, 326. [3]. Pieters *et al.*, (2009), *Science*, 326. [4]. Clark, (2009), *Science*, 326. [5]. Colaprete *et al.*, (2010), *Science*, 330. [6]. Honniball *et al.*, *LPSC*, (2018). [7]. Epstein, Taylor Jr, *LPSC*, (1973). [8]. Needham, Kring, (2017), *EPSL*, 478. [9]. Benna *et al.*, (2019), *Nat. Geo.*, 12. [10]. Hood, Schubert, (1980), *Science*, 208. [11]. Hemingway, Garrick - Bethell, (2012), *JGR*, 117. [12]. Kramer *et al.*, (2011), *JGR*, 116. [13]. Li, Milliken, (2017), *Science Adv.*, 3. [14]. Green *et al.*, (2011), *JGR*, 116. [15]. Tsunakawa *et al.*, (2015), *JGR*, 120. [16]. Bandfield *et al.*, (2018), *Nat. Geo.*, 11. [17]. Wöhler *et al.*, (2017), 285. [18]. McCord *et al.*, (2011), *JGR*, 116. [19]. Li, Garrick - Bethell, (2019), *GRL*, <https://doi.org/10.1029/2019GL084890>. [20] Garrick-Bethell I. *et al.* (2019), *LPS 50*, abstract 2786.

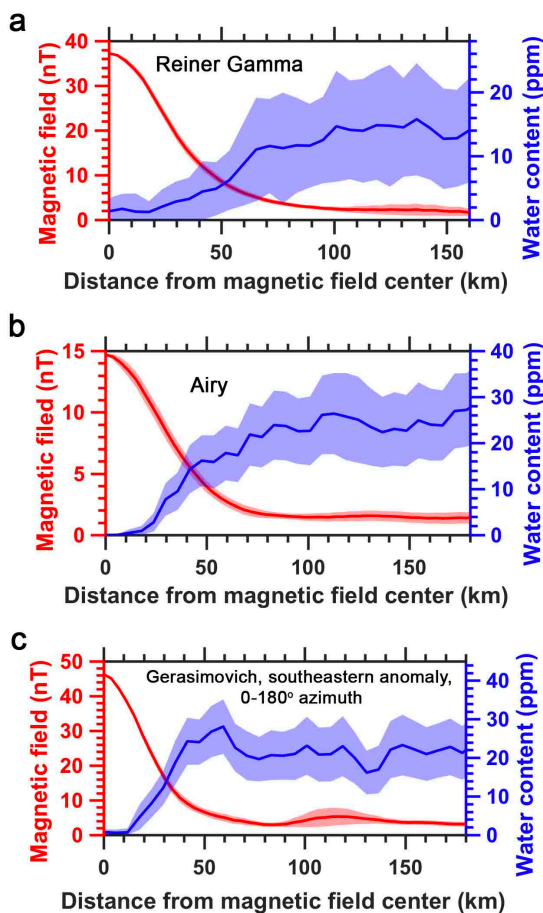


Fig. 2. Azimuthal profiles of averaged water content and magnetic field strength across Reiner Gamma (a), Airy (b), and the southeastern anomaly at Gerasimovich (c), the red and blue shaded regions represent 1 standard deviation of magnetic field and 1/2 standard deviation of water content, respectively. Adapted from Fig. 5 in [19].